Pergamon

Transpn Res.-A, Vol. 32, No. 7, pp. 509–527, 1998

Printed in Great Britain
0965-8564/98 $19.00 + 0.00

PII: S0965-8564(98)00013-5

THE IMPACT OF DRIVER AND FLOW VARIABILITY ON CAPACITY ESTIMATES OF PERMISSIVE MOVEMENTS*

SHANE VELAN and MICHEL VAN AERDE
Department of Civil Engineering, Queen's University, Kingston, Ontario, Canada K7L 3N6

(Received 12 December 1996; in revised form 12 January 1998)

Abstract—The following paper describes a stochastic extension to earlier research into a generalised deterministic model of driver gap acceptance. This gap acceptance model is applicable to traffic flow at both signalised and unsignalised intersections. The proposed microscopic gap acceptance model has been implemented within the INTEGRATION traffic simulation model and is therefore equally suitable for analysis of a single isolated intersection approach for static conditions, as well as in a fully dynamic analysis of networks consisting of hundreds of signalised and unsignalised intersections. Variability in both the supply of gaps in the priority flow and the demand for gaps from the non-priority vehicles is introduced. The analysis illustrates the impact on the overall relationship between priority flow and the capacity of the non-priority flow. Cowan M3 and exponentially distributed gap supply models are considered, as are normal and log-normal gap–demand models which account for driver heterogeneity. The results are not only shown to be logical, but also consistent with several analytical capacity models, the Highway Capacity Manual and a recent National Cooperative Highway Research Program project on the same topic. © 1998 Elsevier Science Ltd. All rights reserved

Keywords: gap acceptance, capacity, permissive movements.

1. INTRODUCTION

All gap acceptance models rely on a gap supply, which determines the variability of the gaps in the higher priority traffic stream, and a gap demand component, which gives an indication of the usefulness of the available gaps to the lower priority traffic stream.

Most previous investigations of microscopic gap acceptance have included either a random gap supply or a stochastic demand for gaps with drivers behaving consistently and/or homogeneously (Plank, 1982; Ashworth and Bottom, 1977; Blumenfeld and Weiss, 1978, 1979). However, usually their combined impact is not quantified adequately. These random and stochastic factors must be analysed individually and collectively, in order to better understand which of these factors have the most significant impact on the ultimate relationship between the priority flow rate, and the capacity or delay of the non-priority flow. Only after the individual impacts of each stochastic factor are understood in isolation, can their rather complex interaction effects be fully understood.

The traditional terminology for describing conflicting flows has been developed for two-way-stop-controlled (TWSC) intersections, where the minor flow on the minor street approach is opposed by the major flow on the major street. However, the application of gap acceptance beyond the TWSC intersection to, for example, yield-controlled intersections and merges, or permitted left turns and right-turns-on-red (RTOR) at signalised intersections, requires a more generalised terminology. Several alternative terminologies have been used in the literature to describe an opposed vehicle on the minor approach, including non-priority vehicle and subject vehicle. Similarly, the priority traffic stream on the major road has been called the priority traffic stream and the conflicting traffic stream. In this paper, a generalised terminology is employed in which a *priority* vehicle is considered to oppose a *non-priority* vehicle.

*Funding for this study was provided by the Natural Sciences and Engineering Research Council of Canada.
†Author for correspondence. Fax: 001 514 481 7473; e-mail: velans@crt.umontreal.ca

This paper demonstrates the steps of implementing stochastic parameters into a uniform supply–demand gap acceptance model (Velan and Van Aerde, 1996a,b). The impact of driver variability on the capacity of a non-priority movement is quantified for a range of priority flow rates on the priority approach. Three parameters are considered for uniform and stochastic conditions:

(a) the distribution of priority traffic stream headways, which act as the supply of gaps;
(b) the distribution of the critical gap of the non-priority vehicles, which is the minimum-length time gap in the priority traffic stream that a non-priority vehicle will accept; and
(c) the distribution of the follow-up time of the non-priority vehicles, which is the time span between the departure of one non-priority vehicle and the departure of the next queued non-priority vehicle, when the priority flow is 0 vph.

The follow-up time is equal to the saturation flow headway of the non-priority approach.

These three binary parameters yield a total of eight (2^3) possible combinations. As it is expected that the distribution of the follow-up time plays a lesser role in determining the capacity of the non-priority approach, the stochastic follow-up time is considered only after the stochastic critical gap and the random headway in the priority traffic stream have been implemented, as indicated in Table 1. The analysis begins with a simplistic scenario of homogeneous non-priority drivers with uniform critical gap and follow-up time, opposed by a uniform priority traffic stream. For this scenario, the capacity of the non-priority approach can be determined readily using analytical techniques. However, as random and stochastic parameters are implemented in the model, the analytical calculations are shown to become increasingly complex and cumbersome. It should be noted that Scenario 3, in which homogeneous and consistent non-priority drivers are opposed by a priority traffic stream with randomly distributed headways, is similar to ch. 10 of the 1994 *Highway Capacity Manual* (HCM) procedure for the estimation of capacity and delay at TWSC intersections.

2. BACKGROUND

Using gap acceptance is the most common and best documented approach for the analysis of capacity and delay at unsignalised intersections. *Intersections without Trafffic Signals* (Brilon, 1988) and *Intersections without Traffic Signals II* (Brilon, 1991) contain a collection of papers from workshops held in Bochum, Germany. National Cooperative Highway Research Program (NCHR-P) Project 3-46, Vol. 1 (Kyte *et al*., 1996) provides recent information concerning the estimation of capacity and delay at unsignalised intersections using gap acceptance models.

2.1. Analytical models for estimating capacity of the non-priority approach

An analytical solution to the capacity of the non-priority approach can be formulated in a general sense as indicated in eqn (1).

$$c = v_p \int_{t=0}^{\infty} f(t)g(t)\mathrm{d}t \tag{1}$$

where

c = non-priority approach capacity (vph)
v_p = priority flow rate (vph),
$f(t)$ = probability distribution of the available gaps, and
$g(t)$ = number of non-priority vehicles which accept a gap of size t seconds.

Table 1. Stages of development of the proposed gap acceptance model with random gap supply and stochastic gap demand

Scenario	Opposing headway	Critical gap	Follow-up time
1	Uniform	Deterministic	Deterministic
2	Uniform	Stochastic	Deterministic
3	Random	Deterministic	Deterministic
4	Random	Stochastic	Deterministic
5	Random	Stochastic	Stochastic

The gap demand function $g(t)$ is controlled by two parameters, the critical gap (t_c) and follow-up time (t_f). Unlike the follow-up time, the critical gap cannot be measured directly in the field. Many procedures have been developed for the estimation of the critical gap based on observations of accepted and rejected gaps. Brilon (1995) used a simulation program to generate accepted and rejected gaps. He compared the estimated critical gaps from many estimation procedures to those values that were used to generate the simulated data. Headways in the priority traffic stream were generated according to the hyper-erlang distribution, and the critical gaps and follow-up times were generated according to a shifted-Erlang distribution with no decay of the critical gap. Two cases with different speeds on the major approach were used to test the effectiveness of the critical gap estimation procedures (1) speed 50 kph, mean critical gap 5.8 s, mean follow-up time 2.6 s and (2) speed 70 kph, mean critical gap 7.2 s, mean follow-up time 3.6 s. For both cases the coefficient of variation (COV) of the critical gap was 0.308 and the COV of the follow-up time was 0.387. Of the estimation procedures tested, including the logit model and methods by Troutbeck (1992), Ashworth (1970), Raff (1950), Harders (1976), Hewitt (1992) and Siegloch (1973), only the maximum likelihood method by Troutbeck (1992) and the probit estimation by Hewitt (1992) gave realistic estimates for the mean critical gap that were independent of the major street volume.

In order to determine recommended values for the critical gap and follow-up time, 59 videotaped periods of operation at 53 unsignalised intersections were recorded and compiled for NCHRP Project 3-46 (Kyte *et al.*, 1996). Recommended values of the mean critical gap for passenger cars varied between 4.1 and 7.5 s, depending on the non-priority movement (left turn, through or right turn) and the number of lanes in the priority traffic stream. The recommended mean follow-up time for passenger cars ranged from 2.2 to 4.0 s, depending on the movement of the non-priority vehicle. Further analysis of the compiled data from NCHRP Project 3-46 (Tian *et al.*, 1995) revealed that the COV of the critical gap varied from 0.29 to 0.41 and the COV of the follow-up time varied from 0.23 to 0.39, depending on the movement of the non-priority vehicle.

Many parameters affect the demand for gaps, ranging from vehicle characteristics and the geometry of the intersection, to driver aggressiveness and familiarity with the intersection (Kyte *et al.*, 1996). These variable parameters are ignored when drivers are assumed to behave homogeneously and consistently. Plank (1982) defines the assumptions of homogeneous and consistent drivers. A deterministic critical gap in which all gaps greater than the critical gap are rejected and all gaps smaller than the critical gap are accepted would imply that a driver is consistent, and if all drivers have the same critical gap then they are homogeneous. Representing the critical gap with a stochastic distribution for a particular driver would imply inconsistent behaviour. If drivers have different values of the critical gap or different stochastic distributions of the critical gap then they are considered to be heterogeneous.

Although most models assume homogeneous and consistent drivers, Ashworth and Bottom (1977) revealed that permitting inconsistent drivers was more realistic than permitting heterogeneity among a group of drivers, since the major source of variability in gap acceptance is within drivers and not between them. Studies by Kittelson and Vandehey (1991) and Kyte *et al.* (1991), which described driver inconsistency, concluded that the critical gap may be expected to decay as a non-priority driver waits at the front of the queue. The error induced by assuming homogeneity was quantified by Blumenfelid and Weiss (1978, 1979), who have shown that assuming drivers are homogeneous leads to an over estimation of capacity, which is unlikely to exceed the true capacity by more than 15%.

When stochastically modelling the critical gap and the follow-up time, the distribution of the variability must be taken into account. Kyte *et al.* (1996) intimated that a stochastic distribution for the critical gap, which can be determined based on data of accepted and rejected gaps, should be characterised by

1. a minimum value as the lower threshold which is greater than zero;
2. an expectation of average critical gap (or mean critical gap);
3. a standard deviation; and
4. a skewness factor, expected to be positive, that assumes and accounts for a longer tail on the right side of the distribution.

The NCHRP Project 3-46 recommendation of the maximum likelihood method (Troutbeck, 1992) as the estimation procedure for the critical gap, which assumes a log-normal distribution, is consistent with the above characteristics.

Historically, the first analytical models for estimating the non-priority approach capacity required several simplifying assumptions, such as a uniform critical gap and follow-up time, and a constant priority flow rate. Harders (1968) and Drew (1968) made two further assumptions to generate their analytical estimation of the non-priority approach capacity (c), as indicated in eqn (2). Their fourth assumption was that an exponential distribution could represent the headways of the priority traffic stream, while a fifth assumption considered that a stepwise function could describe $g(t)$.

$$c = \frac{v_p e^{-v_p t_c}}{1 - e^{-v_p t_f}} \tag{2}$$

Siegloch (1973) retained the first four assumptions, but assumed a continuous linear function for $g(t)$ instead of a stepwise function, to arrive at the alternative model that is presented in eqn (3):

$$c = \frac{1}{t_f} e^{-v_p t_0} \tag{3}$$

where $t_0 = t_c - t_f/2$.
The estimation of the capacity of the non-priority approach was further improved by Tanner (1967), Troutbeck (1986) and Cowan (1987) by assuming that the priority headways followed the Cowan M3 distribution (Cowan, 1975). This assumption modifies the exponential distribution of headways in the non-priority traffic stream to account for bunching of the vehicles. The resulting capacity estimates would follow a formula similar to eqn (4):

$$c = \frac{\alpha v_p e^{-\lambda(t_c - t_m)}}{1 - e^{-\lambda t_f}} \tag{4}$$

where

t_m = minimum inter-vehicle tracking headway of the priority vehicles (s),
α = the proportion of priority vehicles travelling with headways greater than t_m and

$$\lambda = \frac{\alpha v_p/3600}{1 - t_m v_p/3600} = \text{decay constant} \tag{5}$$

As part of NCHRP Project 3-46, extensive data collection was used to test the effectiveness of many analytical models and simulation tools. It was found that accurate delay estimation cannot easily be attained without first modelling capacity accurately. Harders' analytical model and the 1994 HCM procedure for estimating capacity at TWSC intersections could predict the same level of service for 50% of cases, and to within one level of service in 90% of cases. As a result, NCHRP Project 3-46 suggested using simulation for estimating the non-priority approach capacity for complex scenarios. Of the simulation models tested, only KNOSIMO (Grossmann, 1988) accurately estimated the delay at American sites, but it was noted that the model does not capture the effects of multiple lanes.

Given the above context, the remainder of this paper describes the gap acceptance model present within the INTEGRATION traffic simulation model and its relevant attributes.

3. DEVELOPMENT OF A STOCHASTIC GAP ACCEPTANCE MODEL

The INTEGRATION model (Van Aerde and Yagar, 1988a,b; Van Aerde, 1995; Van Aerde and Hellinga, 1996) was used as the platform for the development of a flexible gap-acceptance model based on the following model features. Intersections can have up to seven legs, each of which can be either uncontrolled, yield-controlled, stop-controlled or signalised. Each approach can have up to seven lanes, with striping that permits or prohibits left-turn, through or right-turn movements on each lane. Turning bays and channelisation can be added on any approach. The arrival profiles of all intersection approach flows can be controlled by altering the departure rate, the degree of

randomness of the departure headways, and upstream controls to create platoons. Only after the basic gap acceptance model has been validated, can the more complex model capabilities be used effectively.

For simple modeling of the conflicting traffic streams at an unsignalised intersection INTEGRATION requires several user inputs. The first component of input variables describes the roads, also called links. The jam density, flow at capacity, free speed, speed-at-capacity, and speed variability define the macroscopic speed-flow relationship and the microscopic car-following logic for each link. (See Scenario 3 for further discussion.) The link length and number of lanes will also affect the car-following logic. The downstream control (yield sign, stop sign or signal) must be specified to determine the priority, or hierarchy, of flows at the downstream intersection. In addition, the COV and mean base value of the critical gap, and the critical gap decay constant are specified either globally or for a particular link; adjustment factors are then automatically applied to account for non-priority turning movements, the presence of a stop sign on the non-priority approach and multiple lanes in the priority traffic stream, such that the mean critical gap is consistent with the 1994 HCM. (Further discussion of the critical gap and follow-up time is included in Scenarios 1 and 2.) The second component of input variables specifies each flow demand as an origin-destination pair. Each O–D pair is described by an average flow rate in vehicles per hour (vph), simulation start and end times, a passenger car equivalency, and a proportion of random departure headways. (The implications of these parameters on the departure and arrival headway distributions are discussed in Scenario 3.) Other input components are signal timings and incidents, which are not relevant to this study.

The complex model features and detailed input specifications, together with the dynamic and network features, make the INTEGRATION traffic simulation model an ideal platform for exploring the gap acceptance process of conflicting flows. In addition, the implementation and validation of a gap acceptance model within INTEGRATION improves the accuracy of large scale simulations of networks. The following five sections describe the implementation and simulation results for each of the five scenarios that were considered in the development of a gap acceptance model with random gap supply and stochastic gap demand.

4. SCENARIO 1: UNIFORM GAP SUPPLY AND DETERMINISTIC GAP DEMAND

A simple but fundamental starting point is a scenario in which the priority traffic stream is discharged with uniform headways, and where the demand for these gaps is considered to be deterministic by assuming that the non-priority drivers behave consistently and homogeneously. Specifically, consistency is ensured by assigning a critical gap decay constant of 0.0, so that a non-priority driver always has the same critical gap while waiting at the front of the queue. To achieve homogeneity, all non-priority drivers are considered to have the same critical gap (t_c) of 5.0 s and follow-up time (t_f) of 2.0 s. The follow-up time also implies an unopposed saturation flow rate of 1800 vph (3600 s h^{-1}/2 s veh^{-1}) on the non-priority approach. The values of the critical gap and follow-up time were chosen with two objectives: (a) to be within or close to the range of values recommended by NCHRP Project 3-46 (Kyte *et al.*, 1996) and (b) to simplify the analytical calculations.

4.1. Analytical model

Given that the headways in the priority traffic stream are uniform, the probability distribution of the gap size is given by

$$f(t) = \begin{cases} 1.0 \text{ for } t = 3600/v_p \\ 0.0 \text{ for } t \neq 3600/v_p \end{cases} \tag{6}$$

In this deterministic gap acceptance model, $g(t)$ is a stepwise function with the form

$$g(t) = \max\left(0, 1 + \text{int}\left[\frac{t - t_c}{t_f}\right]\right) \tag{7}$$

where

$\text{int}(x)$ = the nearest integer less than x, and

$\text{int}\left[\dfrac{t - t_c}{t_f}\right]$ = the number of follow-up vehicles for a gap of size t.

Thus, for a gap $t = 3600/v_p$, according to eqn (1) the capacity of the non-priority approach is given by eqn (8). The results of the calculations appear in Table 2.

$$c = v_p \max\left(0, \text{int}\left[\frac{3600/v_p - t_c}{t_f}\right]\right) \tag{8}$$

When the priority flow rate is 0 vph, the available gap is infinitely long, and the non-priority approach capacity is limited only by its saturation flow rate. However, when a priority vehicle nears the conflict zone, the 4.99 s before its arrival are unusable to a non-priority vehicle at the stop line. If the queued non-priority vehicle had been making its way to the stop line, though, up to 2.0 s would not have been useable to the non-priority approach anyway, and a net loss of only 3.0 s due to opposition would result.

In the case of uniform headways in the priority traffic stream, the priority traffic stream contains a series of equally spaced vehicles. Therefore, the non-priority approach is confronted with uniform gaps, which are consistently accepted or rejected by the same number of vehicles. For example, when the priority flow rate is 240 vph, each available gap in the priority traffic stream is equal to 15.0 s (3600 s h^{-1}/240 veh h^{-1}). Consider that this gap is made available at time 100 s. The non-priority vehicle waiting at the stop line accepts the gap, and others follow at 2.0 s intervals, until six vehicles have passed through the gap at times 100, 102, 104, 106, 108, and 110 s. The driver of the next non-priority vehicle arrives at the stop line at 112 s to see that the priority vehicle is only 3.0 s from the conflict zone, which is less than the minimum acceptable gap of 5.0 s. This is consistent with the analytical formulation of $g(t)$ because $g(15) = \max(0, 1 + 5)$. Therefore, six non-priority vehicles discharge every 15 s, producing a capacity of 1440 vph (6 veh/15 s * 3600 s h^{-1}).

Table 2. Summary of the analytically derived capacity of a non-priority approach with $t_c = 5.0$ *s* and $t_f = 2.0$ *s* (Scenario 1)

Priority flow rate, v_p (vph) or (gaps h^{-1})	Gap size, t (s)	Gap acceptance, $g(t)$ (veh gap^{-1})	Blocked time (s gap^{-1})	Non-priority approach capacity, c (vph)
0	∞	∞	0	1800
↓	↓	↓	↓	↓
211	17.06	7	3.06	1477
212	16.98	6	4.98	1272
↓	↓	↓	↓	↓
240	15.00	6	3.00	1440
241	14.94	5	4.94	1205
↓	↓	↓	↓	↓
276	13.04	5	3.04	1380
277	12.996	4	4.996	1108
↓	↓	↓	↓	↓
327	11.01	4	3.01	1308
328	10.98	3	4.98	984
↓	↓	↓	↓	↓
400	9.00	3	3.00	1200
401	8.98	2	4.98	802
↓	↓	↓	↓	↓
514	7.003	2	3.003	1028
515	6.94	1	4.94	515
↓	↓	↓	↓	↓
720	5.00	1	3.00	720
721	4.99	0	4.99	0
↓	↓	↓	↓	↓
1800	2.00	0	2.00	0

Alternatively, the capacity can be derived by the transparency technique described by Plank (1982), in which the capacity is equal to the product of the transparency (the proportion of time the priority traffic stream is not blocking the non-priority approach) and the saturation flow rate of the non-priority approach. Since 3.0 s are lost to the non-priority approach out of every 15 s, the non-priority approach capacity is 1440 vph (12 s/15 s*1800 vph). This 3.0 s is referred to as the *blocked time* of the non-priority approach.

If one now considers a 1 vph increase to the priority flow rate from 240 vph to 241 vph, each gap in the priority traffic stream is now 14.94 s long (3600 s h^{-1}/241 vph). As before, the non-priority vehicle at the stop line accepts the gap which becomes available at time 100 s, and the next four non-priority vehicles follow at intervals of 2 s. But, when the sixth non-priority vehicle arrives at the stop line at time 110 s, only a 4.94 s lag is available, which must be rejected as it is less than the critical gap of 5.0 s. So only five non-priority vehicles can accept each gap, $g(14.94) = \max(0, 1 + 4)$. Thus, with only a 1 vph increase to the priority flow rate, the non-priority approach capacity has fallen abruptly from 1440 to 1205 vph, computed as either five vehicles accepting gaps every 14.94 s (5 veh/14.94 s*3600 s h^{-1}), or 4.94 s of blocked time and 10 s of unblocked time every 14.94 s at the saturation flow rate of 1800 vph(10 s/14.94 s*1800 vph).

As the priority flow rate increases to 276 vph, the blocked time of the non-priority approach decreases from 4.94 s to 3.04 s per available gap, allowing the non-priority approach capacity to increase. Although the gaps are smaller (13.04 versus 14.94 s), five non-priority vehicles will still be able to accept each gap, $g(13.04) = \max(0, 1 + 4)$. Since the gaps are arriving more frequently, the non-priority approach capacity increases linearly with the priority flow rate, and the slope is equal to the number of vehicles accepting each gap in the priority traffic stream. Eventually, another drop in capacity will occur at a priority flow rate of 277 vph, when only four vehicles will be able to accept each 12.996 s gap, and the blocked time will increase to 4.996 s per gap.

This process of a gradual linear increase in the non-priority approach capacity, followed occasionally by abrupt decreases continues, until a priority flow rate of 721 vph is reached. At this point each available gap is 4.99 s, which is too small for even a single non-priority vehicle to accept it. The end points of these abrupt changes are listed in Table 2, and a graph of this discontinuous function is represented in Fig. 1.

4.2. Simulation results

The identical scenario to the one considered above was simulated using the gap acceptance model imbedded in INTEGRATION. Results are presented in Fig. 1. It is clear that the simulation results of the non-priority approach capacity concur with the analytical calculations. It should be noted that this graph was generated using 15 min observations for each priority flow rate. Caution should be exercised when interpolating between the sampled simulation results, since a straight line fails to capture the true stepwise nature of the function.

This scenario is most interesting from a theoretical standpoint, since the case of consistent and homogeneous drivers accepting uniform gaps is not realistic. However, this scenario does serve as a good starting point to understand the fundamental operation of this supply–demand gap acceptance model. Given this base scenario, the implementation of stochastic demand for gaps and/or random supply of gaps can now be considered, as is shown in subsequent sections.

5. SCENARIO 2: UNIFORM GAP SUPPLY AND PARTLY STOCHASTIC GAP DEMAND

The next step in the development of the model consisted of an analysis of the effect of a stochastic critical gap. Since the follow-up time remained uniform, the gap demand side of the model can only be considered partially stochastic.

5.1. Implementation

In Scenario 2, non-priority drivers are still assumed to be consistent, but the homogeneity assumption has been relaxed by modelling the critical gaps of all the non-priority drivers with a log-normal distribution, defined by the mean critical gap and COV. Each non-priority driver's critical gap is assigned based on the driver's aggressiveness, with a more aggressive driver having a

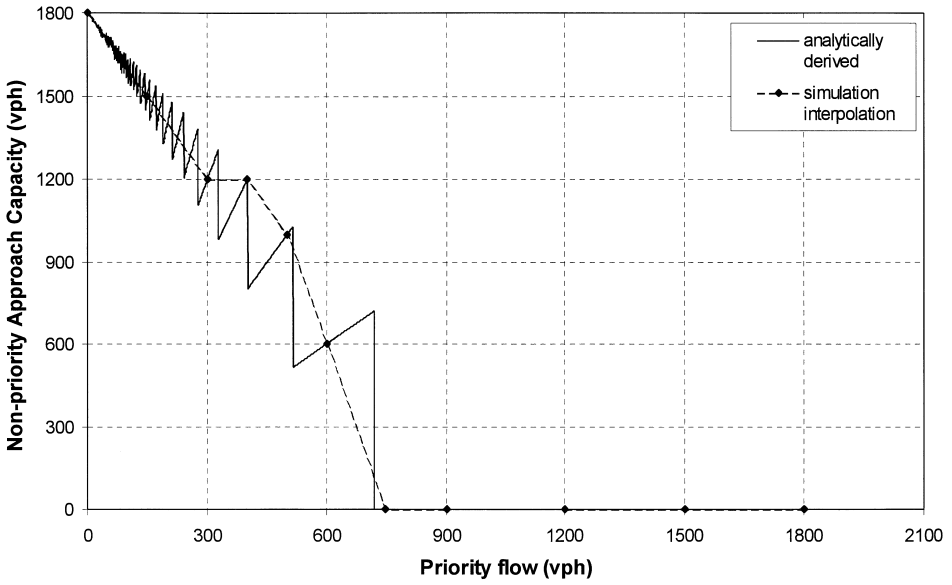

Fig. 1. Analytically derived and simulated non-priority approach capacity under uniform gap supply and deterministic gap demand (Scenario 1: $t_c = 5.0$ s; $t_f = 2.0$ s).

smaller critical gap. Because the critical gap decay parameter is still 0.0, each driver's critical gap remains consistent for the entire duration of their front-of-queue position.

The log-normal distribution was selected to represent the probability density function of the critical gap because it satisfies most of the characteristics as defined by Kyte *et al.*, (1996). Although characteristic (1) is not satisfied by the log-normal distribution since the minimum critical gap is zero, the probability of very small critical gaps is relatively small. The log-normal distribution is a good candidate for modelling the critical gap because it is mathematically simple and tractable.

In this scenario, the critical gaps of the non-priority vehicles were considered to fit a log-normal distribution with a specified mean critical gap of 5.0 s and a COV which was varied from 0.0 to 0.5, which brackets the COVs that were found in the NCHRP Project 3-46 Working Paper no. 16 (Tian *et al.*, 1995).

5.2. *Analytical model*

The probability distribution of the available gaps remained unchanged from Scenario 1, where $f(t)$ is defined by eqn (6). With stochastic gap-demand the front-of-queue non-priority driver will accept an available gap of size t if his/her critical gap is smaller. Since the critical gap is log-normally distributed among all drivers, the probability of the gap acceptance, i.e. $P(t > t_c)$, can be given by the cumulative distribution function of the log-normal distribution, $H(t)$. From Fig. 2 it can be noted that as the critical gap COV increases, the distribution of $H(t)$ becomes flatter and more skewed.

If the front-of-queue vehicle does accept the available gap, then the next queued vehicle will advance to the stop-line exactly 2.0 s later ($t_f = 2.0$ *s*), and the probability of accepting the lag is $H(t + t_f)$. The probability of the nth queued vehicle accepting the lag is equal to $H(t + (n-1)t_f)$, provided that all preceding vehicles do indeed accept the gap. Therefore, the number of vehicles accepting each gap can be given by

$$g(t) = H(t) + \sum_{i=1}^{\infty}\left[\prod_{j=0}^{i} H(t + j.t_f)\right] \tag{9}$$

This formulation of $g(t)$ assumes that each available gap can be treated as an independent event, an assumption that will be compared to the simulation results in the following section. From Fig. 3, it can be seen that the stepwise nature of $g(t)$ is preserved for small critical gap COV, but $g(t)$ becomes a smooth curve for COV greater than 0.3. Also, as the COV increases so does the

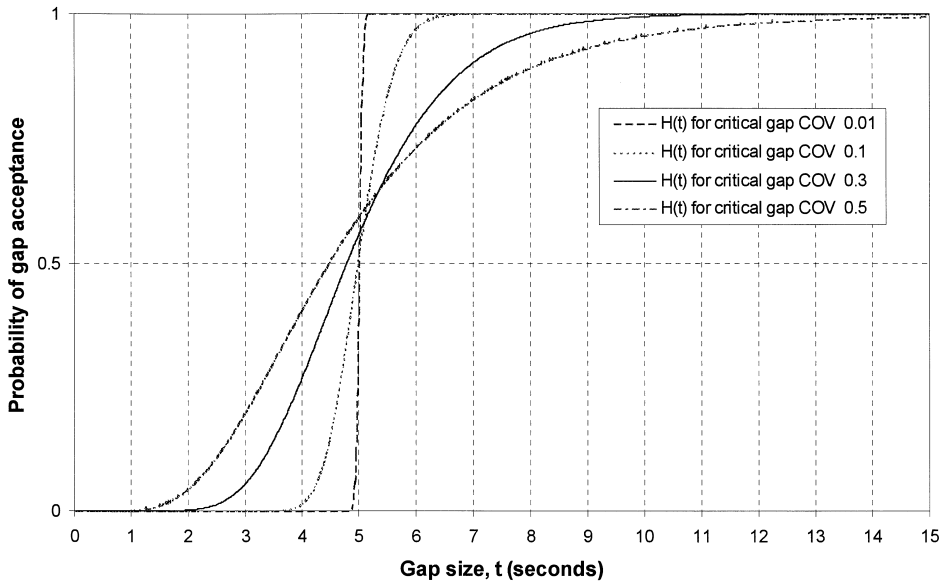

Fig. 2. Probability of acceptance of the available gap t for the front-of-queue non-priority vehicle (Scenario 2: $t_c = 5.0$ s; $t_f = 2.0$ s).

likelihood of the occurrence that a preceding queued vehicle with a critical gap larger than the lag will block all subsequent vehicles from accepting the lag. Consequently, the $g(t)$ tends to decrease with increasing critical gap COV.

Using eqn (1) the capacity can be analytically derived by substituting the functions $f(t)$ and $g(t)$ defined above. The curves in Fig. 4 show that the stepwise nature of the non-priority approach capacity described in Scenario 1 is preserved for small critical gap COV; the curves become smooth for COV greater than 0.3. Also, the tails of the capacity curves for a priority flow rate exceeding 720 vph (3600 s h^{-1}/t_c) correspond to the portion of $g(t)$ where the available gap t is smaller than the critical gap, $t_c = 5.0$ *s*. Finally, it should be noted that increases to the critical gap COV result in increases to the non-priority approach capacity at high priority flows and slight decreases to the capacity at low priority flows. The latter observation does not agree with Blumenfeld and Weiss (1978, 1979), who found that relaxing the homogeneity assumption can result

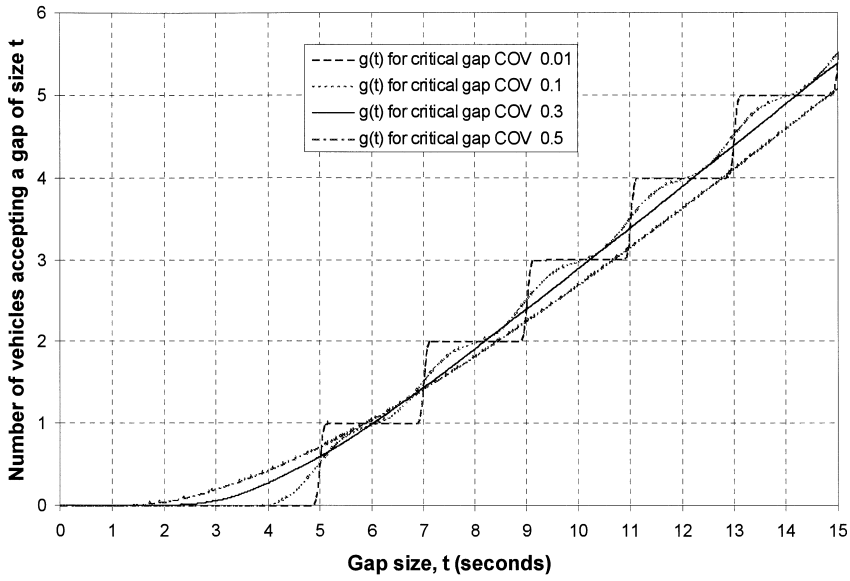

Fig. 3. Mean number of non-priority vehicles that will accept an available gap t (Scenario 2: $t_c = 5.0$ s; $t_f = 2.0$ s).

in estimates of the non-priority approach capacity that are up to 15% smaller than the case of homogeneous drivers with deterministic critical gaps as in Scenario 1 (COV = 0.0).

5.3. Simulation results

Figure 5 shows 15 1-min observations of the non-priority approach for a series of priority flow rates. Non-priority drivers are assumed to be consistent and heterogeneous. The follow-up time is 2.0 s, and the mean critical gap is 5.0 s with COV equal to 0.5.

When the priority traffic stream is flowing uniformly, there is no variability in the priority flow rate from one 1-min observation to the next. Because vehicles are modelled discretely in this microscopic simulation, only an integer number of priority vehicles can be observed for a priority flow rate in any given time interval. For example, for a priority flow rate of 400 vph, or 6.67 vehicles per min, only 6 or 7 vehicles may be observed in any 1-min observation, corresponding to flows of 360 and 420 vph, respectively. So, in Fig. 5 there is no variability in the priority flow *rate* (x-direction), although the 1-min priority flow *observations* may appear in two columns since the measurements were discrete.

If all of the non-priority vehicles reacted in the same way to the uniform available gap, the stepwise nature of Fig. 1 would be preserved. However, with a variable critical gap, non-priority vehicles do not behave homogeneously, resulting in a variance in the non-priority approach capacity from one 1-min observation to the next. In Fig. 5 with COV equal to 0. 5, variance about the stepwise function was present in the y-direction, with the greatest variation for priority flow rates from 300 to 500 vph. This variation in the y-direction tends to smooth the stepwise function seen in Fig. 1.

The non-priority approach has been modelled to operate under oversaturated conditions, so for each priority flow rate the average of the 15 1-min observations of non-priority flow represents a 15-min observation of the capacity. It is apparent from Fig. 4 that the 15-min, non-priority approach capacity is not the same as the analytically derived capacity. For priority flow rates greater than 500 vph, the simulation capacity is smaller than the capacity derived by the analytical procedure because the simulation does not treat every available gap in the priority traffic stream as an independent event. This discrepancy is zero for deterministic critical gaps (COV = 0) and increases with increasing COV.

In the analytical model, it is assumed that for each new gap in the priority traffic stream an independent critical gap is selected from the log-normal distribution. In the simulation, each non-priority driver must be served at the front of the queue before any subsequent non-priority

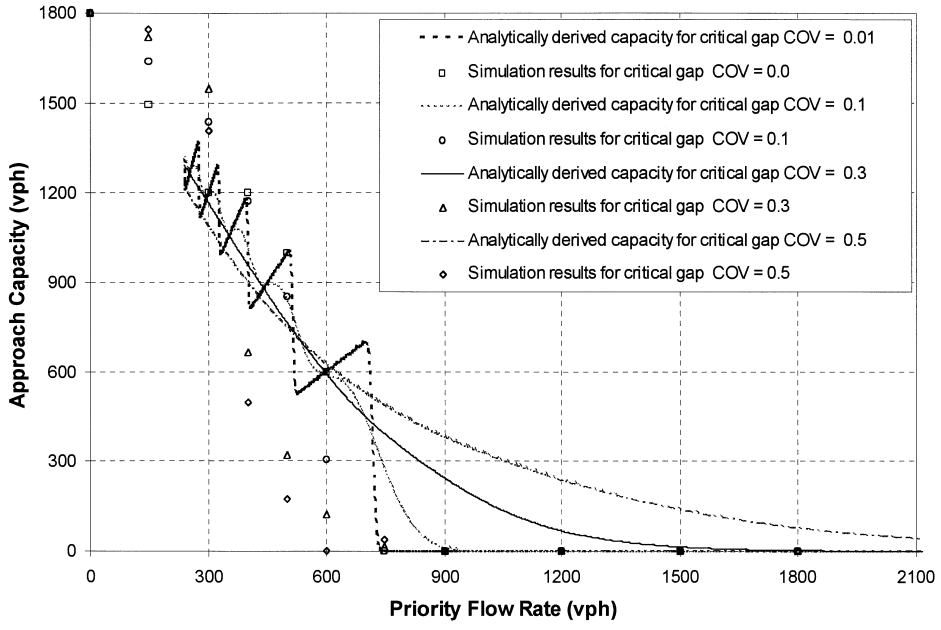

Fig. 4. Capacity for a non-priority approach facing a priority traffic stream (Scenario 2: $t_c = 5.0$ s; $t_f = 2.0$ s).

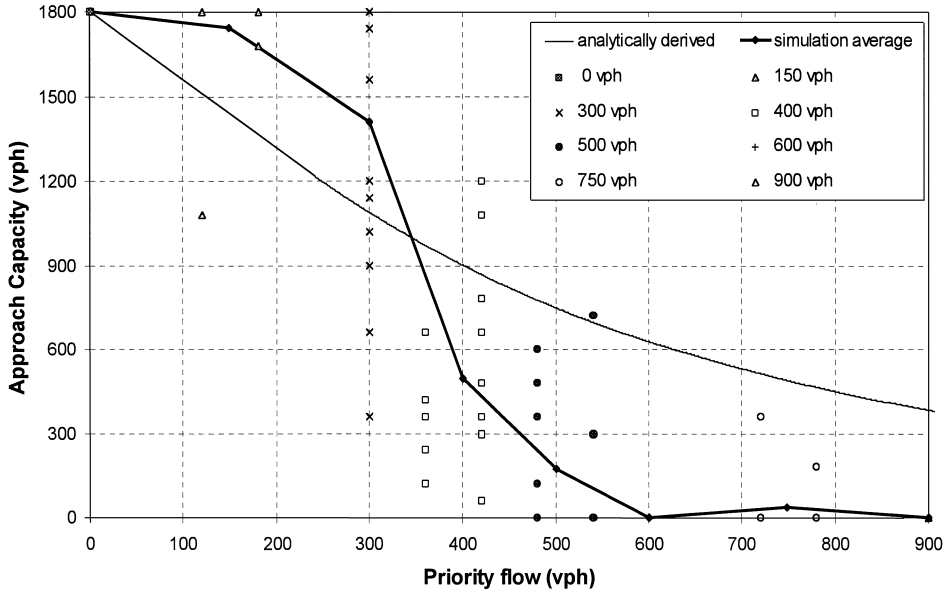

Fig. 5. Variability of the 15 1-min observations for gap acceptance with uniform gap supply and stochastic gap demand (Scenario 2: mean $t_c = 5.0$ s, COV = 0.5; $t_f = 2.0$ s).

vehicles can accept a gap. If a non-priority driver with a critical gap greater than the available gap reaches the front of the queue, that driver will act like a plug on the downstream end of the link, effectively blocking all flow on the non-priority approach for the remainder of the 15-min simulation. This *plug factor* occurs when the front-of-queue driver has a critical gap that is larger than the available gap, which is more likely to occur when the priority flow rate or the critical gap COV increase.

The presence of the plug factor for the entire 15 min duration of the simulation accounted for the non-priority approach capacity of 0 vph at priority flow rates of 900 vph and greater (Fig. 4). In Fig. 5, for a priority flow of 750 vph, six non-priority drivers accepted gaps during the first minute of simulation, producing data point (720 vph, 360 vph); 3 non-priority drivers accepted gaps during the second 1-min observation, producing data point (780 vph, 180 vph); and no more gaps were accepted for the remainder of the simulation due to the plug factor. This created a 15-min observation of capacity equal to 36 vph, compared to the analytical estimate of 487 vph.

The simulated values agree with Blumenfeld and Weiss (1978, 1979), except that the capacity reductions are often greater than 15% and they do not apply for all priority flow rates. The impact of the plug factor would be reduced if the drivers behaved inconsistently, by modelling the critical gap with decay. Then the front-of-queue vehicle would eventually discharge no matter how large the initial critical gap was. To see the impact of the critical gap decay with strictly deterministic critical gaps, see Velan and Van Aerde (1996a,b).

A second factor which causes non-priority approach capacity increases for small priority flow rates remains unexplained. It is clear that this factor has a greater impact on the non-priority approach capacity for increased critical gap COV. At the time of publication, the authors were unable to explain the capacity increases, although there is a suspicion that the car-following logic is the cause of the discrepancy between the analytical estimates and simulation values.

6. SCENARIO 3: RANDOM GAP SUPPLY AND DETERMINISTIC GAP DEMAND

This third scenario considers all non-priority drivers to be consistent and homogeneous, but variability is introduced into the headways of the priority traffic stream. This scenario has been modelled extensively through analytical methods, and matches the assumptions of the 1994 HCM. The analytical capacity models discussed earlier by Harders (1976), Siegloch (1973) and Troutbeck (1986) are utilised in this section to verify the simulation results.

6.1. Implementation

The INTEGRATION model permits the user to specify the level of randomness in the trip departure headways from each trip origin as being from 0 to 100% random. If, for a flow of 900 vph, the randomness was specified as 0%, the departure headways would all have a uniform length of 4.0 s (3600 s h^{-1}/900 vph). In contrast, if the model user requested 100% randomness, the mean departure headway remains 4.0 s, but the standard deviation would be equal to the mean, according to the mathematical properties of the exponential distribution. For 50% randomness, each vehicle's departure headway consists of a constant portion equal to 2.0 s, plus a random component with a mean and standard deviation of 2.0 s.

As the priority vehicles with random headways travel along the priority approach from their trip origin, the distribution of headways may be affected by the prevailing microscopic car-following logic. This logic captures the relationship between each vehicle's speed with its individual headway (Van Aerde, 1995). During the simulation, each vehicle determines its speed based on the current distance headway each decisecond, according to the formula

$$h_d = c_1 + \frac{c_2}{u_f - u} + c_3 u \tag{10}$$

where

h_d = distance headway (km)
u = speed (km h^{-1})
dimensionless constant, $k = c_1/c_2 = (2u_c - u_f)/(u_f - u_c)^2$
first variable distance headway constant $(km^2\, h^{-1})$, $c_2 = 1/(d_j(k + 1/u_f))$
fixed distance headway constant (km), $c_1 = kc_2$
second variable distance headway constant (h^{-1}), $c_3 = u_c^{-1}(-c_1 + u_c/q_c - c_2/(u_f - u_c))$
flow at capacity, $q_c = 1800$ vph
free speed, $u_f = 60$ km h^{-1}
speed-at-capacity, $u_c = 55$ km h^{-1}
jam density, $d_j = 140$ veh km^{-1}

The distinction between the randomness of the departure headways of the priority traffic stream and a platooned priority traffic stream may need clarification. Velan and Van Aerde (1996a) considered platooned flow due to upstream signals separately from randomness of the departure headways of the priority traffic stream.

6.2. Simulation results

As a result of the car-following logic, vehicles that start with larger than average headways at the upstream end of the priority approach, travel at a somewhat greater speed, thereby reducing their headway relative to the preceding vehicle on the link. In contrast, vehicles that start their trip with a smaller than average headway will initially reduce their speed, which in turn increases their headway relative to the preceding vehicle on the link. The impact of the former gap-shrinking effect was minimised by specifying a speed-at-capacity (55 km h^{-1}) that was close to the free-speed (60 km h^{-1}) and by limiting the priority approach to 500 m in length. The latter gap-expanding effect created a noticeable change in the proportion of small headways in the priority traffic stream, as seen in Fig. 6.

For a priority flow rate of 900 vph and 100% random departure headways, Fig. 6 displays (a) the cumulative departure headway distribution of the priority traffic stream 500 m upstream of the unsignalised intersection and (b) the cumulative arrival headway distribution of the priority traffic stream at the unsignalised intersection, i.e. after the effects of car-following on the priority approach. Fig. 7 shows the same cumulative headway distributions for a flow of 1740 vph and 100% randomness, which is close to the priority approach capacity of 1800 vph.

The departure headways tend to follow the negative exponential distribution quite closely, with a mean headway of 4.0 s for priority flow 900 vph (3600 s h^{-1}/900 vph = 4.0 s) and mean headway 2.07 s for priority flow 1740 vph (3600 s h^{-1}/1740 vph = 2.07 s). The car-following logic eliminated all headways smaller than the minimum time headway of 2.0 s ($1/q_c$), and increased the proportion of headways greater than 2.0 s.

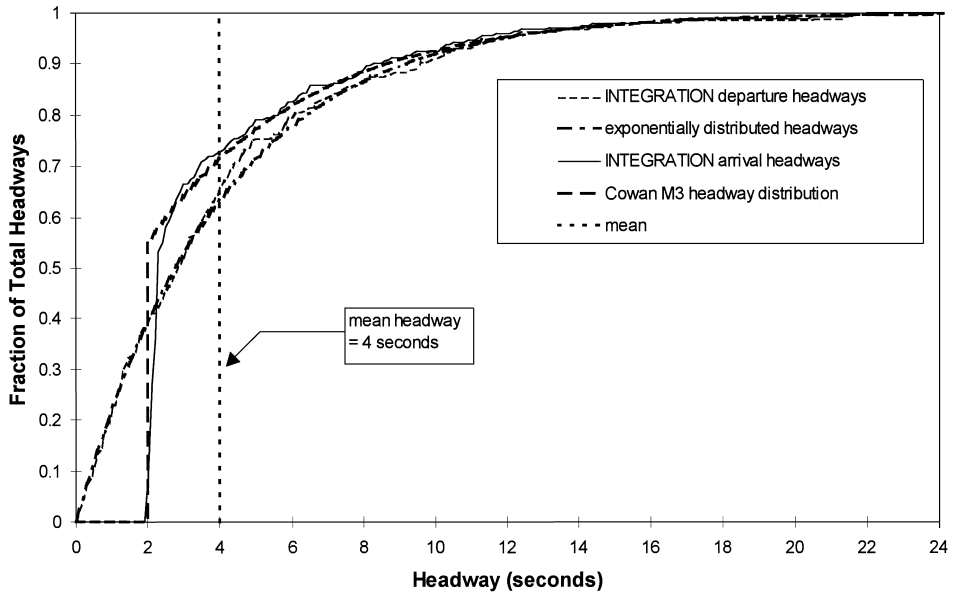

Fig. 6. Distribution of departure and arrival headways in the priority traffic stream at a priority flow rate of 900 vph.

The arrival headways tend to follow the Cowan M3 distribution, a dichotomised distribution in which a proportion of the vehicles travel in bunches and the remaining vehicles travel with free headways corresponding to a shifted negative exponential distribution. The probability distribution function $f(t)$ and the cumulative distribution function $F(t)$ for the Cowan M3 distribution are

$$f(t) = \begin{cases} 0 & \text{for } t < t_m \\ 1-\alpha & \text{for } t = t_m \\ \alpha\lambda e^{-\lambda(t-t_m)} & \text{for } t < t_m \end{cases} \tag{11}$$

$$F(t) = \begin{cases} 0 & \text{for } t < t_m \\ 1-\alpha e^{-\lambda(t-t_m)} & \text{for } t \geqslant t_m \end{cases} \tag{12}$$

where α, λ and t_m are as defined previously.

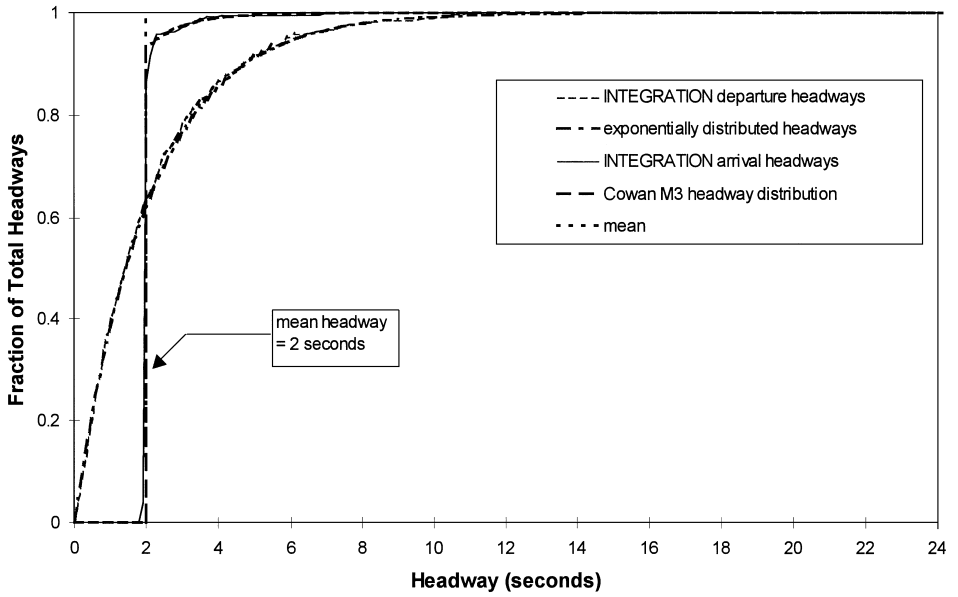

Fig. 7. Distribution of departure and arrival headways in the priority traffic stream at a priority flow rate of 1800 vph.

The Cowan M3 distribution was calibrated to the simulation arrival headways by first setting t_m, the minimum inter-vehicle tracking headway of the priority vehicles, to the inverse of the flow at capacity ($1/q_c$). Then α, the proportion of priority vehicles travelling with headways greater than t_m, was adjusted until the Cowan M3 cumulative distribution function visually matched the simulation cumulative arrival headways. The calibrated values of α were 0.45 for 900 vph and 0.07 for 1740 vph, meaning that 55 and 93% of the priority vehicles were travelling at the minimum headway, respectively.

As seen in Figs 6 and 7, the exponential distribution, which is used to reflect the headway distribution in the Harders (1976) and Siegloch (1973) models, does not account for a minimum following distance. Clearly, the simulated arrival headway distribution does not fit the exponential distribution for any arrival headway smaller than 10 s. In the simulation, the minimum headway actually has an associated variability which would cause the arrival headway distribution to better fit the more realistic Cowan M4 distribution (Cowan, 1975). Since all available gaps that are smaller than the critical gap will be rejected by the non-priority vehicles, obtaining the correct distribution for the very small headways in the priority traffic stream is not crucial anyway.

Fig. 8 provides a series of curves which represent the capacity of the non-priority approach for varying levels of randomness in the departure headways of the priority traffic stream. It can be noted that an increase in the randomness of headways in the priority traffic stream produced increases in the capacity of the non-priority approach. Specifically, compared to uniform priority flow as was the case in Scenario 1 (0% randomness), on average the non-priority approach capacity increased by 35 vph for 25% randomness, by 80 vph for 5% randomness, by 135 vph for 75% randomness, and by 175 vph for 100% randomness. While the capacity of the non-priority approach was reduced by the presence of smaller than average gaps, this reduction was more than offset by the greater number of follow-up vehicles which would accept each large gap.

The Troutbeck (1986), Harders (1976) and Siegloch (1973) capacity models were used to estimate the non-priority approach capacity for the case of 100% random departure headways, the case where the arrival headways will most closely match the exponential distribution. The Troutbeck model assumes that the arrival headways of the priority traffic stream, which are also the available gaps, can be represented by the Cowan M3 distribution, which must be calibrated for varying priority flow rates as was done above. Rather than calibrating α for all simulated priority arrival headways, the value of α was estimated by linear interpolation between intercepts (0 vph, 1.00) and (1800 vph, 0.00), and the previously calibrated points (900 vph, 0.55) and (1740 vph, 0.07).

These results match the Troutbeck model more closely than the estimation of the capacity from the Harders and Siegloch models. Compared to 100% random flow, on average the non-priority

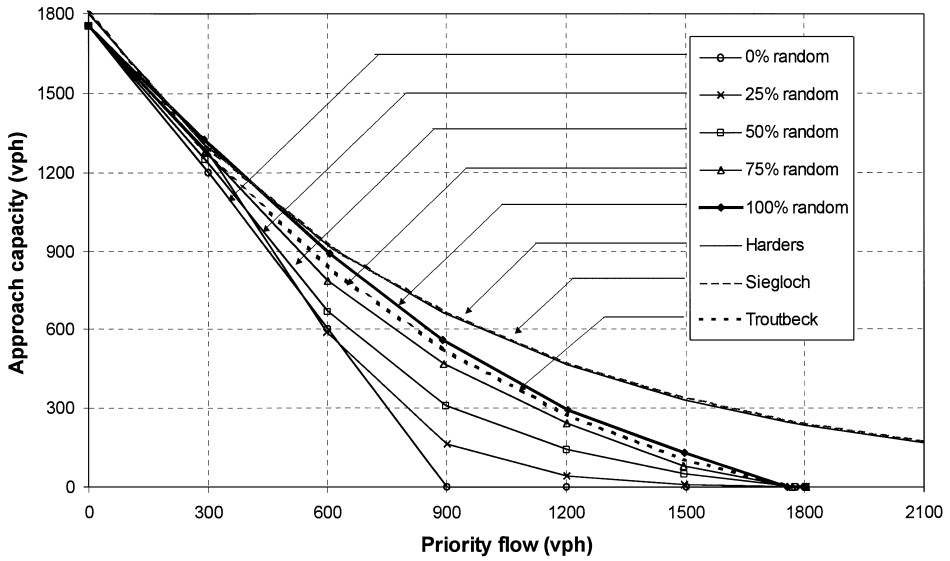

Fig. 8. Impact of randomness in the departure headways in the priority traffic stream on the non-priority approach capacity with uniform gap demand (Scenario 3: $t_c = 5.0$ s; $t_f = 2.0$ s).

approach capacity was 30 vph different from the Troutbeck model's estimation, whereas the Harders and Siegloch models had average discrepancies of 129 vph and 135 vph, respectively. In the Harders and Slegloch models, the use of the exponential distribution to represent the headway distribution of the priority traffic stream permits impossibly small headways; consequently, large gaps in the priority traffic stream become available to the non-priority vehicles, even at priority flow rates that exceed the priority approach's saturation flow rate. This explains the asymptotic behaviour of the Harders and Siegloch models along the positive x-axis.

The apparent variability in the 1-min observations should be addressed at this time. As randomness of the non-priority departure headways was increased, the variance of the priority arrival rate increased for the sample of 15 1-min observations. In Fig. 9, one may note that data points with the same *specified* non-priority flow rate often have different *observed* non-priority flow rates, and hence have different x-coordinates. As a result of the variability in headways of the priority traffic stream, both small and large gaps became available to the non-priority vehicles. The number of non-priority vehicles, which accepted each particular gap, depended only on the size of the available gap, since the critical gap and follow-up time were held constant. The apparent variability in the y-direction is somewhat misleading. If an observation was made for each available gap, then all of the data points would fall exactly on the discontinuous function presented in Fig. 1. However, each data point is a 1-min aggregation, thereby creating the appearance of variability in the y-direction in Fig. 9.

7. SCENARIO 4: RANDOM GAP SUPPLY AND PARTLY STOCHASTIC GAP DEMAND

During the following analysis, the level of randomness in departure headways in the priority traffic stream was fixed at 100%, while the critical gap COV was varied from 0.0 to 1.0 (consistent and heterogeneous non-priority drivers). As discussed in Scenario 2, the plug factor tends to decrease the non-priority approach capacity, when a vehicle requiring a large critical gap reaches the front of the queue. The increases in the non-priority approach capacity for low priority flow rates and large critical gap COV remain unexplained.

As shown on Fig. 10, an increased critical gap COV created a more pronounced S-shaped curve. The intercepts remained fixed because the variability of the critical gap and the degree of randomness in the priority flow have no impact on the non-priority approach capacity when the priority flow is 0 vph or if the available gaps are equal to the saturation flow headway of 2 s (3600 s h^{-1}/1800 vph) on the priority approach.

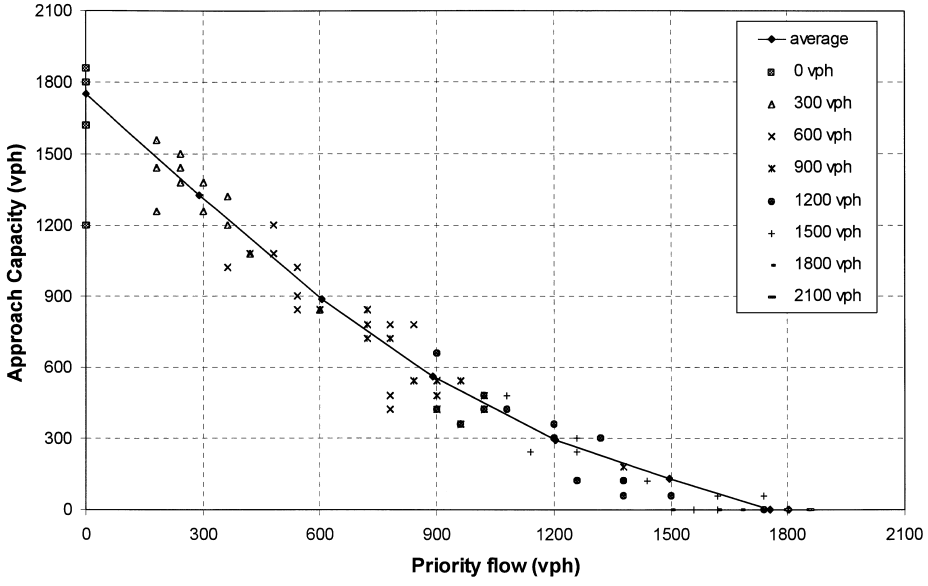

Fig. 9. Variability of 1-min observations of non-priority approach capacity for 100% random departure headways with uniform gap demand (Scenario 3: $t_c = 5.0$ s; $t_f = 2.0$ s).

One important difference between this Scenario 4 and Scenario 2 is that the x-intercept is much larger in Scenario 4. Potentially, with uniform priority flow in Scenario 2, a plug could completely stop the flow of the non-priority approach. However, with random headways in the priority traffic stream it was found that eventually a large gap arrives, allowing the plug to become dislodged.

As discussed in Scenario 3, the random priority flow creates variability in the x-direction for the 1-min observations. As the critical gap COV increased in this scenario, the variability of the 1-min observations of approach capacity also increased in the y-direction due to the plug factor, as explained in Scenario 2. Finally, variability in both the x-direction and y-direction for COV greater than 0.1 has sufficiently obscured the stepwise function such that interpolation between the data points can be regarded as a valid estimate of the average approach capacity.

8. SCENARIO 5: RANDOM GAP SUPPLY AND STOCHASTIC GAP DEMAND

In this final scenario, a truly random supply and stochastic demand gap acceptance model is formulated. In addition to random departure headways in the priority traffic stream and log-normally distributed critical gaps, a stochastic follow-up time (t_f) is introduced.

8.1. Implementation

After a non-priority vehicle accepts a gap and crosses the stop line, the next vehicle in queue proceeds to the stop line at the saturation flow rate (q_c), specified as 1800 vph. Before reaching the stop line, the driver is unable to accept gaps in the priority traffic stream, effectively suspending the gap acceptance process. The time required for that vehicle to proceed to the stop line, commonly referred to as the follow-up time, is equal to the saturation flow rate headway $(1/q_c)$ of 2.0 s. Alternatively, the same time duration may be thought of as the time required for a vehicle to travel the distance of one jam density headway $(1/d_j)$ at the speed-at-capacity (u_c) of the approach, $t_f = \frac{1}{q_c} = \frac{1}{d_j * u_c}$. Therefore, any variability in the jam density or the speed-at-capacity is reflected indirectly in the follow-up time.

INTEGRATION permits the specification of a vehicle speed variability factor, which results in a stochastic speed–headway relationship that dictates the car-following behaviour. The COV of the follow-up time is equal to the COV of the speed-at-capacity.

8.2. Simulation results

The results that are presented next have 100% random headways in the priority traffic stream, and critical gaps that are log-normally distributed, with a mean of 5.0 s and COV set equal to 0.3.

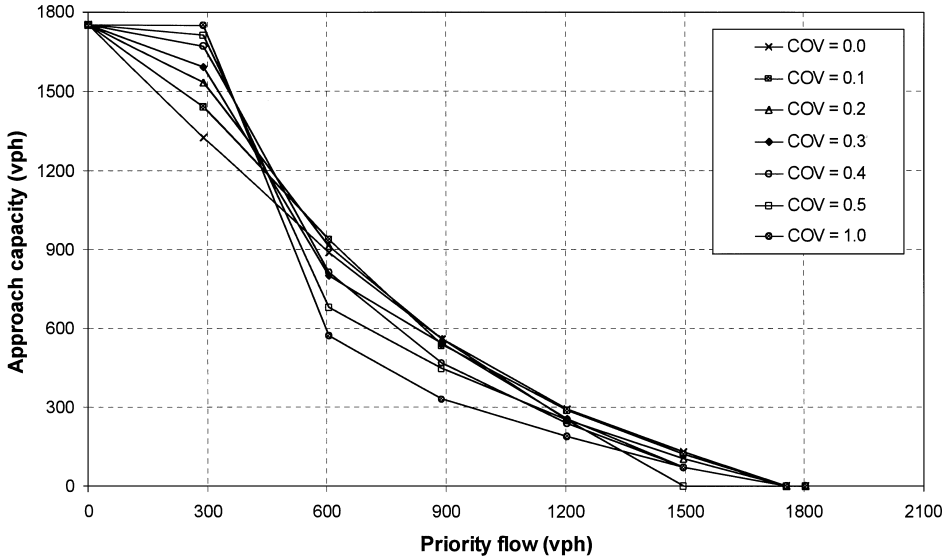

Fig. 10. Impact of the critical gap COV on the non-priority approach capacity with 100% random departure headways in the priority traffic stream (Scenario 4: mean $t_c = 5.0$ s; $t_f = 2.0$ s).

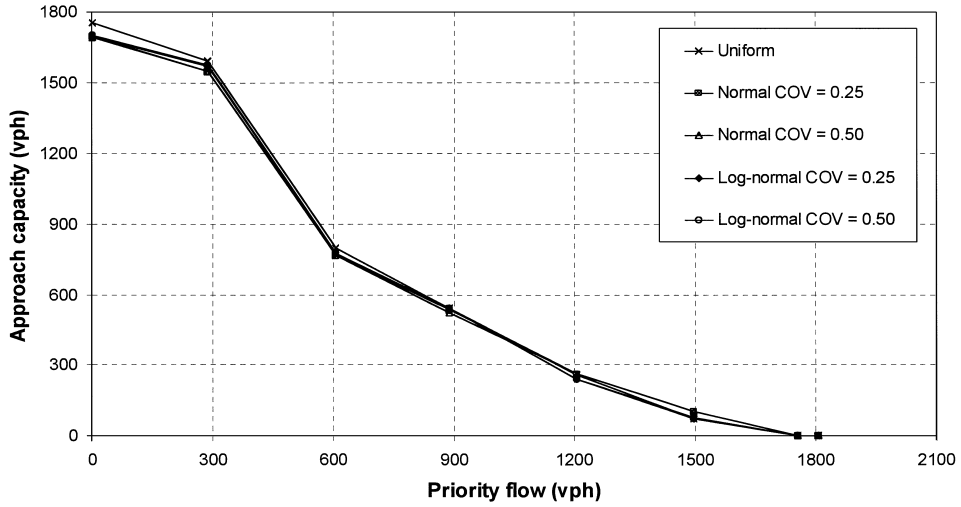

Fig. 11. Impact of the distribution and variance of the follow-up time on the non-priority approach capacity with 100% random departure headways in the priority traffic stream and stochastic critical gap (Scenario 5: mean $t_c = 5.0$ s, COV = 0.3; mean $t_f = 2.0$ s).

The vehicle speed variability was modelled using a COV set equal to 0.25 and 0.50, and both the normal and log-normal distributions were considered. Data from NCHRP Project 3-46 (Tian *et al.*, 1995) confirm that these values and ranges are reasonable. The simulation results are presented in Fig. 11.

Increases in the COV of the follow-up time were shown to have no appreciable impact on the non-priority approach capacity for both the normal and log-normal distributions. Instead, it was found that when a vehicle with a large follow-up time becomes the front of the queue, it may not reach the stop line with enough time to accept a gap, whereas a vehicle with the mean follow-up time may have been able to discharge. Likewise, a vehicle with a follow-up time smaller than the mean may accept a gap that produces an increase in the non-priority approach capacity. However, unlike other pairs of asymmetric, offsetting factors in gap acceptance, these two factors appear to exactly balance each other. In effect, the gap acceptance process is suspended while the follow-up time occurs. Whether these suspensions occur in equal units of 2.0 s, for example, or as variable time lengths with an average of 2.0 s does not change the sum of the time intervals when gap acceptance is suspended.

Therefore, the reduction in the capacity of the non-priority approach (y-intercept of Fig. 11), which is attributable to the follow-up time, is considered to be dependent only on the mean follow up time and not its distribution. Nevertheless, this feature should still be incorporated into this gap acceptance model since it captures a realistic part of the variability in driver behaviour. Also, the variability of the follow-up time may become significant as the interactions with other factors are considered.

9. CONCLUSIONS

Analysis of all five scenarios in the development of the gap acceptance model with random gap supply and stochastic gap demand yielded the following conclusions.

A gap acceptance model with uniform gap supply and deterministic gap demand (Scenario 1) has a stepwise relationship between non-priority approach capacity and priority flow rate, with no variability from one 1-min observation to the next. A gap acceptance model with uniform gap supply and partly stochastic gap demand (Scenario 2) has no variance in the priority flow rate, but it does have variability in the non-priority approach capacity from one 1-min observation to the next. In Scenario 2, the plug factor decreased the non-priority approach capacity, especially at large priority flow rates, which is in agreement with Blumenfeld and Weiss (1978, 1979), except that the capacity reductions are often greater than 15% and they do not apply for all priority flow rates.

A gap acceptance model with random gap supply and deterministic gap demand (Scenario 3) has variability in the priority flow rate. The deterministic critical gap and follow-up time result in the same stepwise function $g(t)$ for the number of vehicles accepting a gap of size t. Overall, the non-priority approach capacity increases for increasing randomness in the headways—as opposed to uniform headways—of the priority traffic stream. INTEGRATION's arrival headway distribution was a better fit to the Cowan M3 headway distribution than the exponential distribution; consequently, the non-priority approach capacity predicted by the simulation matched the Troutbeck model more closely than the Harders model or the Slegloch model.

A gap acceptance model with random gap supply and partly stochastic gap demand (Scenario 4) has variability in both the priority flow rate and the non-priority approach capacity. The variability is sufficient to produce a smooth curve of non-priority approach capacity vs priority flow rate. In Scenario 4, the plug factor decreased the non-priority approach capacity for priority flows greater than 600 vph, with more impact as the critical gap COV was increased. The addition of a stochastic follow-up time (Scenario 5) had no impact on the mean non-priority approach capacity, but the variability which was introduced was more representative of driver behaviour. Analytical models for Scenarios 4 and 5 were found to be cumbersome and impractical.

10. RECOMMENDATIONS

Most analytical models of non-priority approach capacity assume that the impacts of considering drivers to be homogeneous and consistent are equal and offsetting. INTEGRATION's critical gap decay feature can model inconsistent drivers. Capacity estimates with realistic headway distributions of the priority traffic stream and with various combinations of driver inconsistency and heterogeneity could be used to test the assumption made by the analytical models. Before this can be done, the capacity increases (Scenarios 2 and 4) at small priority flow rates for increasing critical gap COV must be corrected or explained.

The simulation model should be tested to verify the non-priority approach capacity for a range of intersection control types and diverse geometric combinations. This simulation model should be applied to scenarios that are difficult to model analytically, for example intersections with two stage gap acceptance. Also, multiple conflicting flows should be considered to assess the resulting impedance and compare those values to the HCM. The evaluation of capacity and estimates of delay should be compared directly to field data to verify the accuracy of this gap acceptance model. This comparison will reveal the most critical calibration factors when this model is applied in the field.

Once the model has been more thoroughly verified, validated and calibrated, it could be used to assess at which critical volumes each intersection control type operates best. From this assessment, which would be performed by one consistent tool, guidelines could be developed which indicate the appropriate control type at a given intersection, and the associated implications on delay, fuel consumption and vehicle emissions.

Acknowledgements—Special thanks to Bruce Robinson from Kittelson and Associates, Inc., as well as the anonymous reviewers of this paper for their comments.

REFERENCES

Ashworth, R. (1970) The analysis and interpretation of gap acceptance data. *Transportation Research* **4**, 270–280.

Ashworth, R. and Bottom, C. G. (1977) Some observations of driver gap-acceptance behavior at a priority intersection. *Traffic Engineering and Control* **18**, 569–571.

Blumenfield, D. E. and Weiss, G. H. Weiss (1978) Statistics of delay for a driver population with step and distributed gap acceptance functions. *Transportation Research* **12**, 423–429.

Blumenfield, D. E. and Weiss, G. H. (1979) The effects of gap-acceptance criteria on merging delay and capacity at an uncontrolled junction. *Traffic Engineering and Control* **20**, 16–20.

Brilon, W. (ed.) (1988) *Intersections Without Traffic Signals, Proceedings of an International Workshop*. Springer-Verlag, Berlin.

Brilon, W. (ed.) (1991) *Intersections Without Traffic Signals II, Proceedings of an International Workshop*. Springer-Verlag, Berlin.

Brilon, W. (1995) Delays at oversaturated unsignalised intersections based on reserve capacities. Presented at the Transportation Research Board 75th Annual Meeting, Paper no. 950013, Washington, DC.

Cowan, R. J. (1975) Useful headway models. *Transportation Research* **9**, 371–375.

Cowan, R. J. (1987) An extension of Tanner's results on uncontrolled intersections: clarification of some issues. *Queuing Systems* **1**, 249–263.

Drew, D. R. (1968) *Traffic Flow Theory and Control*. McGraw-Hill, New York.

Grossmann, M. (1988) KNOSIMO—A practical simulation model for unsignalised intersections. *Intersections Without Traffic Signals, Proceedings of an International Workshop*, pp. 263–273. Springer-Verlag, Berlin.

Harders, J. (1968) The capacity of unsignalised urban intersections. *Schriftenreihe Strassenbau and Strassenverkehrstechnik* **76** (In German).

Harders, J. (1976) Critical gaps and move up times as the basis of capacity calculations for rural roads. *Strassenban and Strassenverherstechnic* **216** (In German).

Hewitt, R. H. (1992) *Using Probit Analysis with Gap Acceptance Data*. Department of Civil Engineering of Glasgow.

Kittelson, W. K. and Vandehey, M. A. (1991) Delay effects on driver gap acceptance characteristics at two-way stop-controlled intersections. *Transportation Research Record* **1320**, 154–159.

Kyte, M., Clemow, C., Mahfood, N., Lall, B. K. and Khisty, C. J. (1991) Capacity and delay characteristics of two-way stop-controlled intersections. *Transportation Research Record* **1320**, 160–167.

Kyte, M., Tian, Z., Mir, Z., Hameedmansoor, Z., Kittelson, W., Vandehey, M., Robinson, B., Brilon, W., Bondzio, L., Wu, N. and Troubeck, R. (1996) *Capacity and Level of Service at Unsignalised Intersections*. National Cooperative Highway Research Program Project 3-46. Transportation Research Board, National Research Council, Washington, DC.

Plank, A. W. (1982) The capacity of a priority intersection-two approaches. *Traffic Engineering and Control* **23**, 88–89.

Raff, M. S. (1950) A *Volume Warrant for Urban Stop Signals*. The Eno Foundation for Highway Traffic Control, Saugatuck, Connecticut.

Siegloch, W. (1973) Capacity calculations for unsignalised intersections. *Schriften-reihe Strassenbau and Strassenverkehrstechnik* **76**, Bonn, West Germany. (In German).

Special Report 209: Highway Capacity Manual (1994) Transportation Research Board, National Research Council, Washington, DC.

Tanner, J. C. (1967) The capacity of an uncontrolled intersection. *Biometrika* **54**, 657–658.

Tian, Z. Troutbeck, R. Brilon, W. Robinson, B. and Kyte, M. (1995) Estimating critical gaps and follow-up times for TWSC intersections. National Cooperative Highway Research Program Project 3-46, working paper 16, Transportation Research Board, National Research Council, Washington, DC.

Troutbeck, R. J. (1986) Average delay at an unsignalised intersection with two major streams each having a dichotomised headway distribution. *Transportation Science* **20**, 272–286.

Troutbeck, R. J. (1992) Estimating the critical acceptance gap from traffic movements. Research report 92-5.

Van Aerde, M. and Yagar, S. (1988) Dynamic integrated freeway/traffic signal networks: problems and proposed solutions. *Transportation Research-A* **22**, 435–443.

Van Aerde, M. and Yagar, S. (1988) Dynamic integrated freeway/traffic signal networks: a routing-based modeling approach. *Transportation Research-A* **22**, 445–453.

Van Aerde, M. (1995) A single regime speed-flow-density relationship for freeways and arterials. Transportation Research Board 75th Annual Meeting, Washington, DC.

Van Aerde, M. and Hellinga, B. (1996) INTEGRATION: overview of current simulation features. Transportation Research Board 75th Annual Meeting. Paper no. 961082, Washington, DC.

Velan, S. and Van Aerde, M. (1996*a*) Relative effects of opposing flow and gap acceptance characteristics on approach capacity at uncontrolled intersections. Transportation Research Board 75th Annual Meeting, Washington, DC.

Velan, S. and Van Aerde, M. (1966) Gap acceptance and approach capacity at unsignalised intersections. *ITE Journal* **66**(3), 40–45.